
Learning MDPs from Features: Predict-Then-Optimize for Sequential Decision Problems by Reinforcement Learning

Anonymous Author(s)

Affiliation

Address

email

Abstract

1 In the predict-then-optimize framework, the objective is to train a predictive model,
2 mapping from environment features to parameters of an optimization problem,
3 which maximizes decision quality when the optimization is subsequently solved.
4 Recent work on decision-focused learning shows that embedding the optimization
5 problem in the training pipeline can improve decision quality and help generalize
6 better to unseen tasks compared to relying on an intermediate loss function for
7 evaluating prediction quality. We study the predict-then-optimize framework in the
8 context of *sequential* decision problems (formulated as MDPs) that are solved via
9 reinforcement learning. In particular, we are given environment features and a set
10 of trajectories from training MDPs, which we use to train a predictive model that
11 generalizes to unseen test MDPs without trajectories. Two significant computa-
12 tional challenges arise in applying decision-focused learning to MDPs: (i) large
13 state and action spaces make it infeasible for existing techniques to differentiate
14 through MDP problems, and (ii) the high-dimensional policy space, as parameter-
15 ized by a neural network, makes differentiating through a policy expensive. We
16 resolve the first challenge by sampling provably unbiased derivatives to approxi-
17 mate and differentiate through optimality conditions, and the second challenge by
18 using a low-rank approximation to the high-dimensional sample-based derivatives.
19 We implement both Bellman-based and policy gradient-based decision-focused
20 learning on three different MDP problems with missing parameters, and show that
21 decision-focused learning performs better in generalization to unseen tasks.

22 1 Introduction

23 *Predict-then-optimize* [4, 8] is a framework for solving optimization problems with unknown param-
24 eters. Given such a problem, we first train a predictive model to predict the missing parameters from
25 problem features. Our objective is to maximize the resulting decision quality when the optimization
26 problem is subsequently solved with the predicted parameters [24, 26]. Recent work on the *decision-*
27 *focused learning* approach [6, 34] embeds the optimization problem [1–3] into the training pipeline
28 and trains the predictive model end-to-end to optimize the final decision quality. Compared with a
29 more traditional “two-stage” approach which maximizes the predictive accuracy of the model (rather
30 than the final decision quality), the decision-focused learning approach can achieve a higher solution
31 quality and generalize better to unseen tasks.

32 This paper studies the predict-then-optimize framework in *sequential* decision problems, formulated
33 as Markov decision processes (MDPs), with unknown parameters. In particular, at training time, we
34 are given trajectories and environment features from “training MDPs.” Our goal is to learn a predictive
35 model which maps from environment features to missing parameters based on these trajectories that

36 generalizes to unseen test MDPs that have features, but not trajectories. The resulting “predicted”
37 training and test MDPs are solved using deep reinforcement learning (RL) algorithms, yielding
38 policies that are then evaluated by offline off-policy evaluation (OPE) as shown in Figure 1. This fully
39 offline setting is motivated by real-world applications such as wildlife conservation and tuberculosis
40 treatment where no simulator is available. However, such domains offer past ranger patrol trajectories
41 and environmental features of individual locations from conservation parks for generalization to other
42 unpatrolled areas. These settings differ from those considered in transfer-RL [20, 23, 27, 29] and
43 meta-RL [7, 9, 31, 33, 38] because we generalize across different MDPs by explicitly predicting
44 the mapping function from features to missing MDPs parameters, while transfer/meta RL achieve
45 generalization by learning hidden representation of different MDPs implicitly with trajectories.

46 The main contribution of this paper is to extend the decision-focused learning approach to MDPs with
47 unknown parameters, embedding the MDP problems in the predictive model training pipeline. To
48 perform this embedding, we study two common types of optimality conditions in MDPs: a Bellman-
49 based approach where mean-squared Bellman error is minimized, and a policy gradient-based
50 approach where the expected cumulative reward is maximized. We convert these optimality conditions
51 into their corresponding Karush–Kuhn–Tucker (KKT) conditions, where we can backpropagate
52 through the embedding by differentiating through the KKT conditions. However, existing techniques
53 from decision-focused learning and differentiating through KKT conditions do not directly apply as
54 the size of the KKT conditions of sequential decision problems grow linearly in the number of states
55 and actions, which are often combinatorial or continuous and thus become intractable.

56 We identify and resolve two computational challenges in applying decision-focused learning to
57 MDPs, that come up in both optimality conditions: (i) the large state and action spaces involved in
58 the optimization reformulation make differentiating through the optimality conditions intractable
59 and (ii) the high-dimensional policy space in MDPs, as parameterized by a neural network, makes
60 differentiating through a policy expensive. To resolve the first challenge, we propose to sample
61 an estimate of the first-order and second-order derivatives to approximate the optimality and KKT
62 conditions. We prove such a sampling approach is unbiased for both types of optimality conditions.
63 Thus, we can differentiate through the approximate KKT conditions formed by sample-based deriva-
64 tives. Nonetheless, the second challenge still applies—the sampled KKT conditions are expensive
65 to differentiate through due to the dimensionality of the policy space when model-free deep RL
66 methods are used. Therefore, we propose to use a low-rank approximation to further approximate the
67 sample-based second-order derivatives. This low-rank approximation reduces both the computation
68 cost and the memory usage of differentiating through KKT conditions.

69 We empirically test our decision-focused algorithms on three settings: a grid world with unknown
70 rewards, and snare-finding and Tuberculosis treatment problems where transition probabilities are
71 unknown. Decision-focused learning achieves better OPE performance in unseen test MDPs than two-
72 stage approach, and our low-rank approximations significantly scale-up decision-focused learning.

73 Related Work

74 **Differentiable optimization** Amos et al. [2] propose using a quadratic program as a differentiable
75 layer and embedding it into deep learning pipeline, and Agrawal et al. [1] extend their work to convex
76 programs. Decision-focused learning [6, 34] focuses on the predict-then-optimize [4, 8] framework
77 by embedding an optimization layer into training pipeline, where the optimization layers can be
78 convex [6], linear [21, 34], and non-convex [25, 32]. Unfortunately, these techniques are of limited
79 utility for sequential decision problems because their formulations grow linearly in the number of
80 states and actions and thus differentiating through them quickly becomes infeasible. Amos et al. [2]
81 avoid this issue by studying model-predictive control but limited to quadratic-form actions, reducing
82 the dimensionality. Karkus et al. [15] differentiate through an algorithm by unrolling and relaxing
83 all the strict operators by soft operators. Futoma et al. [10] deal with large optimality conditions by
84 differentiating through the last step of the value-iteration algorithm only. Instead, our approach does
85 not rely on any MDP solver structure. We combine sampling and a low-rank approximation to form
86 an unbiased estimate of the optimality conditions to differentiate through, and show that the approach
87 of Futoma et al. [10] is included in ours as a special case.

88 **Predict-then-optimize and offline reinforcement learning** The idea of planning under a predicted
89 MDP arises in model-based RL as *certainty equivalence* [18]. It has been extended to offline

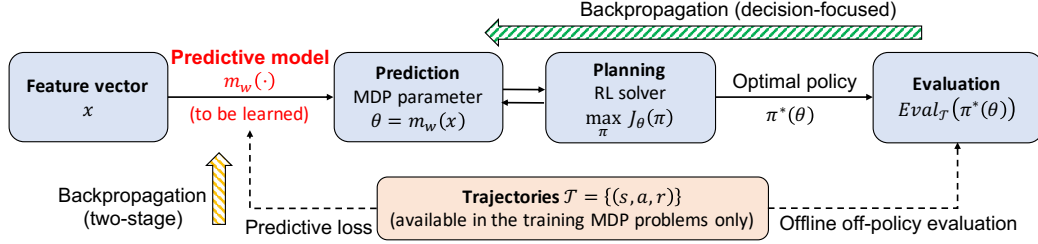


Figure 1: We consider learning a predictive model to map from features to unknown MDP parameters and obtaining a policy by solving the predicted MDP with RL. Two-stage learning learns the predictive model by minimizing a predictive loss function, whereas decision-focused learning is trained end-to-end to maximize the final off-policy evaluation performance.

90 settings [16, 37], who learn a pessimistic MDP before solving for the policy. Our setting differs
 91 because of the presence of features and train-test split—our test MDPs are completely fresh *without*
 92 *any trajectories*. Our setting also resembles meta RL (e.g., [7, 9, 31, 33, 38]) and transfer RL (e.g.,
 93 [20, 23, 27, 29].) Meta RL focuses on training a “meta policy” for a distribution of tasks (MDPs),
 94 leveraging trajectories for each. Transfer RL works by extracting transferable knowledge from source
 95 MDPs to target MDPs using trajectories. In contrast to these two paradigms, ours explicitly trains a
 96 predictive model (which maps problem features to missing MDP parameters) to generalize knowledge
 97 learned from the training set to the testing set using *problem features, not trajectories*.

98 2 Problem Statement

99 In this paper, we consider learning a predictive model to infer the missing parameters in a sequential
 100 decision-making task (formulated as MDPs) using the predict-then-optimize framework. Each MDP
 101 is defined by a tuple $(S, s_0, \mathcal{A}, T, R)$ with an initial state s_0 , a possibly infinite state space S and
 102 possibly infinite action space \mathcal{A} . We assume some parameters are missing in each MDP, which
 103 could be any portion of the transition function T and the reward function R . We denote the missing
 104 parameters vector by θ^* . Additionally, we assume there are problem features x associated with each
 105 MDP, where (θ^*, x) is correlated and drawn from the same unknown, but fixed, distribution.

106 We are given a set of training MDPs and a set of test MDPs, each with missing parameters θ^* and
 107 features x . Each training MDP is accompanied by a set of trajectories \mathcal{T} performed by a behavior
 108 policy π_{beh} , consisting of a sequence of states, actions and rewards. In the test MDPs, trajectories
 109 are hidden at training time. Thus, at training time, we learn a predictive model m_w to map from
 110 features to missing parameters; at test time, we apply the same model to make predictions and plan
 111 accordingly without using trajectories.

112 Formally, our goal is to learn a predictive model m_w to predict the missing parameters $\theta = m_w(x)$.
 113 The predicted parameters are used to solve the test MDPs, yielding the policy $\pi^*(m_w(x))$ where our
 114 offline off-policy evaluation (OPE) metric is maximized. This framework is illustrated in Figure 1.

115 **Offline off-policy evaluation** We evaluate a policy π in a fully offline setting with trajectories
 116 $\mathcal{T} = \{\tau_i\}$, $\tau_i = (s_{i1}, a_{i1}, r_{i1}, \dots, s_{ih}, a_{ih}, r_{ih})$ generated from the MDP using behavior policy π_{beh} .
 117 We use an OPE metric used by Futoma et al. [10] — we evaluate a policy π and trajectories \mathcal{T} as:

$$\text{Eval}_{\mathcal{T}}(\pi) := V^{\text{CWPDIS}}(\pi) - \lambda_{\text{ESS}} / \sqrt{\text{ESS}(\pi)} \quad (1)$$

118 where $V^{\text{CWPDIS}}(\pi) := \sum_{t=1}^h \gamma^t \frac{\sum_i r_{it} \rho_{it}(\pi)}{\sum_i \rho_{it}(\pi)}$ and $\text{ESS}(\pi) := \sum_{t=1}^h \frac{(\sum_i \rho_{it})^2}{\sum_i \rho_{it}^2}$, and $\rho_{it}(\pi)$ is the ratio of
 119 the proposed policy and the behavior policy likelihoods up to time t : $\rho_{it}(\pi) := \prod_{t'=1}^t \frac{\pi(a_{it'} | s_{it'})}{\pi_{\text{beh}}(a_{it'} | s_{it'})}$.

120 **Optimization formulation** Given a set of training features and trajectories $D_{\text{train}} =$
 121 $\{(x_i, \mathcal{T}_i)\}_{i \in I_{\text{train}}}$, our goal is to learn a predictive model m_w to optimize the training performance:

$$\max_w \mathbb{E}_{(x, \mathcal{T}) \in D_{\text{train}}} [\text{Eval}_{\mathcal{T}}(\pi^*(m_w(x)))] \quad (2)$$

122 The testing performance is evaluated on the unseen test set $D_{\text{test}} = \{(x_i, \mathcal{T}_i)\}_{i \in I_{\text{test}}}$ with trajectories
 123 hidden from training, and only used for evaluation: $\mathbb{E}_{(x, \mathcal{T}) \in D_{\text{test}}} [\text{Eval}_{\mathcal{T}}(\pi^*(m_w(x)))]$.

124 **3 Two-stage Learning**

125 To learn the predictive model m_w from trajectories, the standard approach is to minimize an expected
 126 predictive loss, which is defined by comparing the prediction $\theta = m_w(x)$ with the trajectories \mathcal{T} :

$$\min_w \mathbb{E}_{(x, \mathcal{T}) \sim \mathcal{D}_{\text{train}}} \mathcal{L}(\theta, \mathcal{T}) \quad \text{where} \quad \mathcal{L}(\theta, \mathcal{T}) = \mathbb{E}_{\tau \sim \mathcal{T}} \ell_{\theta}(\tau), \quad \theta = m_w(x) \quad (3)$$

127 For example, when the rewards are missing, the loss could be the squared error between the predicted
 128 rewards and the actual rewards we see in the trajectories for each individual step.

129 In the first stage, to train the predictive model, we run gradient descent to minimize the loss function
 130 defined in Equation (3) and make prediction on the model parameter $\theta = m_w(x)$ of each problem. In
 131 the second stage, we solve each MDP problem with the predicted parameter θ using an RL algorithm
 132 to generate the optimal policy $\pi^*(\theta)$. However, predictive loss and the final evaluation metric are
 133 commonly misaligned especially in deep learning problems with imbalanced data [5, 13, 14, 19].
 134 This motivates us to learn the predictive model end-to-end and therefore avoid the misalignment.

135 **4 Decision-focused Learning**

136 In this section, we present our main contribution, decision-focused learning in sequential decision
 137 problems, as illustrated in Figure 1. Decision-focused learning integrates an MDP problem into the
 138 training pipeline to directly optimize the final performance. Instead of relying on a predictive loss
 139 to train the predictive model m_w , we can directly optimize the objective in Equation (2) by running
 140 end-to-end gradient descent to update the predictive model m_w :

$$\frac{d \text{Eval}(\pi^*)}{dw} = \frac{d \text{Eval}(\pi^*)}{d\pi^*} \frac{d\pi^*}{d\theta} \frac{d\theta}{dw} \quad (4)$$

141 We assume the policy $\pi^*(\theta)$ is either stochastic and smooth with respect to the change in the
 142 parameter θ , which is common in settings with continuous state or action spaces, or that an appropriate
 143 regularization term [11, 12] is used to improve the smoothness of the policy.

144 This gradient computation requires us to back-propagate from the final evaluation through the MDP
 145 layer to the predictive model m_w that we want to update. The major challenge in Equation (4) is to
 146 compute $\frac{d\pi^*}{d\theta}$, which involves differentiating through an MDP layer solved by an RL algorithm. In
 147 the following section, we first discuss two different optimality conditions in MDPs, which are later
 148 used to convert into KKT conditions and differentiate through to compute $\frac{d\pi^*}{d\theta}$. We then discuss two
 149 computational challenges associated with the derivative computation.

150 **4.1 Optimality Conditions in MDPs**

151 When the predicted model parameter $\theta = m_w(x)$ is given, the MDP can be solved by any RL
 152 algorithm to get an optimal policy π^* . Here we discuss two common optimality conditions in MDPs,
 153 differing by the use of policy gradient or Bellman equation:

154 **Definition 1** (Policy gradient-based optimality condition). *Defining $J_{\theta}(\pi)$ to be the expected cumu-*
 155 *lative reward under policy π , the optimality condition of the optimal policy π^* is:*

$$\pi^* = \arg \max_{\pi} J_{\theta}(\pi) := \mathbb{E}_{\tau \sim \pi, \theta} G_{\theta}(\tau) \quad (5)$$

156 *where $G_{\theta}(\tau)$ is the discounted value of trajectory τ given parameter θ , and the expectation is taken*
 157 *over the trajectories following the optimal policy and transition probability (as part of θ).*

158 **Definition 2** (Bellman-based optimality condition). *Defining $J_{\theta}(\pi)$ to be the mean-squared Bellman*
 159 *error under policy π , the optimality condition of the optimal policy π^* (valuation function) is:*

$$\pi^* = \arg \min_{\pi} J_{\theta}(\pi) := \mathbb{E}_{\tau \sim \pi, \theta} \frac{1}{2} \delta_{\theta}^2(\tau, \pi) \quad (6)$$

160 *where $\delta_{\theta}(\tau, \pi) = \sum_{(s, a, s') \in \tau} Q_{\pi}(s, a) - R_{\theta}(s, a) - \gamma \mathbb{E}_{a' \sim \pi} Q_{\pi}(s', a')$ is the total Bellman error of*
 161 *a trajectory τ , and $\delta_{\theta}(\tau, \pi)$ depends on the parameter θ because the immediate reward R_{θ} does. The*
 162 *expectation in Equation (6) is taken over all the trajectories generated from policy π and transition*
 163 *probability (as part of θ).*

164 4.2 Backpropagating Through Optimality and KKT Conditions

165 To compute the derivative of the optimal policy $\pi^*(\theta)$ in an MDP with respect to the MDP parameter
166 θ , we differentiate through the KKT conditions of the corresponding optimality conditions:

167 **Definition 3** (KKT Conditions). *Given objective $J_\theta(\pi)$ in an MDP problem, since the policy param-*
168 *eters are unconstrained, the necessary KKT conditions can be written as: $\nabla_\pi J_\theta(\pi^*) = 0$.*

169 In particular, computing the total derivative of KKT conditions gives:

$$\begin{aligned} 0 &= \frac{d}{d\theta} \nabla_\pi J_\theta(\pi^*) = \frac{\partial}{\partial \theta} \nabla_\pi J_\theta(\pi^*) + \frac{\partial}{\partial \pi} \nabla_\pi J_\theta(\pi^*) \frac{d\pi^*}{d\theta} = \nabla_{\theta\pi} J_\theta(\pi^*) + \nabla_\pi^2 J_\theta(\pi^*) \frac{d\pi^*}{d\theta} \\ \implies \frac{d\pi^*}{d\theta} &= -(\nabla_\pi^2 J_\theta(\pi^*))^{-1} \nabla_{\theta\pi} J_\theta(\pi^*) \end{aligned} \quad (7)$$

170 We can use Equation (7) to replace the term $\frac{d\pi^*}{d\theta}$ in Equation (4) to compute the full gradient to
171 back-propagate from the final evaluation to the predictive model parameterized by w :

$$\frac{d \text{Eval}(\pi^*)}{dw} = -\frac{d \text{Eval}(\pi^*)}{d\pi^*} (\nabla_\pi^2 J_\theta(\pi^*))^{-1} \nabla_{\theta\pi} J_\theta(\pi^*) \frac{d\theta}{dw} \quad (8)$$

172 4.3 Computational Challenges in Backward Pass

173 Unfortunately, although we can write down and differentiate through the KKT conditions analytically,
174 we cannot explicitly compute the second-order derivatives $\nabla_\pi^2 J_\theta(\pi^*)$ and $\nabla_{\theta\pi}^2 J_\theta(\pi^*)$ in Equation (8)
175 due to the following two challenges:

176 **Large state and action spaces involved in optimality conditions** The objectives $J_\theta(\pi^*)$ in Defi-
177 nition 1 and Definition 2 involve an expectation over all possible trajectories, which is essentially an
178 integral and is intractable when either the state or action space is continuous. This prevents us from
179 explicitly verifying optimality and writing down the two derivatives $\nabla_\pi^2 J_\theta(\pi^*)$ and $\nabla_{\theta\pi}^2 J_\theta(\pi^*)$.

180 **High-dimensional policy space parameterized by neural networks** In MDPs solved by model-
181 free deep RL algorithms, the policy space $\pi \in \Pi$ is often parameterized by a neural network,
182 which has a significantly larger number of variables than standard optimization problems. This
183 large dimensionality makes the second-order derivative $\nabla_\pi^2 J_\theta(\pi^*) \in \mathbb{R}^{\dim(\pi) \times \dim(\pi)}$ intractable to
184 compute, store, or invert.

185 5 Sampling Unbiased Derivative Estimates

186 In both policy gradient-based and Bellman-based optimality conditions, the objective is implicitly
187 given by an expectation over all possible trajectories, which could be infinitely large when either
188 state or action space is continuous. This same issue arises when expressing such an MDP as a linear
189 program — there are infinitely many constraints, making it intractable to differentiate through.

190 Inspired by the policy gradient theorem, although we cannot compute the exact gradient of the
191 objective, we can sample a set of trajectories $\tau = \{s_1, a_1, r_1, \dots, s_h, a_h, r_h\}$ from policy π and
192 model parameter θ with finite time horizon h . Denoting $p_\theta(\tau, \pi)$ to be the likelihood of seeing
193 trajectory τ , we can compute an unbiased derivative estimate for both optimality conditions:

194 **Theorem 1** (Policy gradient-based unbiased derivative estimate). *We follow the notation of Defini-*
195 *tion 1 and define $\Phi_\theta(\tau, \pi) = \sum_{i=1}^h \sum_{j=i}^h \gamma^j R_\theta(s_j, a_j) \log \pi(a_i | s_i)$. We have:*

$$\nabla_\pi J_\theta(\pi) = \mathbb{E}_{\tau \sim \pi, \theta} [\nabla_\pi \Phi_\theta(\tau, \pi)] \implies \begin{aligned} \nabla_\pi^2 J_\theta(\pi) &= \mathbb{E}_{\tau \sim \pi, \theta} [\nabla_\pi \Phi_\theta \cdot \nabla_\pi \log p_\theta^\top + \nabla_\pi^2 \Phi_\theta] \\ \nabla_{\theta\pi}^2 J_\theta(\pi) &= \mathbb{E}_{\tau \sim \pi, \theta} [\nabla_\pi \Phi_\theta \cdot \nabla_\theta \log p_\theta^\top + \nabla_{\theta\pi}^2 \Phi_\theta] \end{aligned} \quad (9)$$

196 **Theorem 2** (Bellman-based unbiased derivative estimate). *We follow the notation in Definition 2 to*
197 *define $J_\theta(\pi) = \frac{1}{2} \mathbb{E}_{\tau \sim \pi, \theta} [\delta_\theta^2(\tau, \pi)]$. We have:*

$$\begin{aligned} \nabla_\pi J_\theta(\pi) &= \mathbb{E}_{\tau \sim \pi, \theta} \left[\delta \nabla_\pi \delta + \frac{1}{2} \delta^2 \nabla_\pi \log p_\theta \right] \implies \nabla_\pi^2 J_\theta(\pi) = \mathbb{E}_{\tau \sim \pi, \theta} [\nabla_\pi \delta \nabla_\pi \delta^\top + O(\delta)] \\ \nabla_{\theta\pi}^2 J_\theta(\pi) &= \mathbb{E}_{\tau \sim \pi, \theta} [\nabla_\pi \delta \nabla_\theta \delta^\top + (\nabla_\pi \delta \nabla_\theta \log p_\theta^\top + \nabla_\pi \log p_\theta \nabla_\theta \delta^\top + \nabla_{\theta\pi}^2 \delta) \delta + O(\delta^2)] \end{aligned} \quad (10)$$

198 For the latter, we apply the fact that at the near-optimal policy, the Bellman error is close to 0 and
 199 thus each individual component $\delta(\tau, \pi)$ is small to simplify the analysis. Refer to the appendix for
 200 the full derivations of Equations (9) and (10).

201 Equations (9) and (10) provide a sampling approach to compute the second-order derivatives, avoiding
 202 computing an expectation over the large trajectory space. We can use the optimal policy derived
 203 in the forward pass and the predicted parameters θ to run multiple simulations to collect a set of
 204 trajectories. These trajectories from predicted parameters can be used to compute each individual
 205 derivative in Equations (9) and (10).

206 6 Resolving High-dimensional Derivatives by Low-rank Approximation

207 Section 5 provides sampling approaches to compute an unbiased estimate of second-order derivatives.
 208 However, since the dimensionality of the policy space $\dim(\pi)$ is often large, we cannot explicitly
 209 expand and invert $\nabla_{\pi}^2 J_{\theta}(\pi^*)$ to compute $\nabla_{\pi}^2 J_{\theta}(\pi^*)^{-1} \nabla_{\theta}^2 J_{\theta}(\pi^*)$, which is an inevitable step toward
 210 computing the full gradient of decision-focused learning in Equation (8). In this section, we discuss
 211 various ways to approximate $\nabla_{\pi}^2 J_{\theta}(\pi^*)$ and how we use low-rank approximation and Woodbury
 212 matrix identity [35] to efficiently invert the sampled Hessian without expanding the matrices. Let
 213 $n := \dim(\pi)$ and $k \ll n$ to be the number of trajectories we sample to compute the derivatives.

214 6.1 Full Hessian Computation

215 In Equations (9) and (10), we can apply auto-differentiation tools to compute all individual derivatives
 216 in the expectation. However, this works only when the dimensionality of the policy space $\pi \in \Pi$
 217 is small because the full expressions in Equations (9) and (10) involve computing second-order
 218 derivatives, e.g., $\nabla_{\pi}^2 \Phi_{\theta}$ in Equation (10), which is still challenging to compute and store when the
 219 matrix size $n \times n$ is large. The computation cost is $O(n^2) + O(n^{\omega})$, where $2 \leq \omega \leq 2.373$ is the
 220 complexity order of matrix inversion.

221 6.2 Approximating Hessian by Constant Identity Matrix

222 One naive way to approximate the Hessian $\nabla_{\pi}^2 J_{\theta}(\pi^*)$ is to simply use a constant identity matrix cI .
 223 We choose $c < 0$ for the policy gradient-based optimality in Definition 1 because the optimization
 224 problem is a maximization problem and thus is locally concave at the optimal solution, whose
 225 Hessian is negative semi-definite. Similarly, we choose $c > 0$ for the Bellman-based optimality in
 226 Definition 2. This approach is fast, easily invertible. Moreover, in the Bellman version, Equation (8)
 227 is equivalent to the idea of differentiating through the final gradient of Bellman error as proposed by
 228 Futoma et al. [10]. However, this approach ignores the information provided by the Hessian term,
 229 which can often lead to instability as we later show in the experiments. In this case, the computation
 230 complexity is dominated by computing $\nabla_{\theta}^2 J_{\theta}(\pi^*)$, which is of size $O(nk)$.

231 6.3 Low-rank Hessian Approximation and Application of Woodbury Matrix Identity

232 A compromise between the full Hessian and using a constant matrix is approximating the second-
 233 order derivative terms in Equations (9) and (10) by constant identity matrices, while computing the
 234 first-order derivative terms with auto-differentiation. Specifically, given a set of k sampled trajectories
 235 $\{\tau_1, \tau_2, \dots, \tau_k\}$, Equations (9) and (10) can be written and approximated in the following form:

$$\nabla_{\pi}^2 J_{\theta}(\pi) \approx \frac{1}{k} \sum_{i=1}^k (u_i v_i^{\top} + H_i) \approx \frac{1}{k} \sum_{i=1}^k (u_i v_i^{\top} + cI) = UV^{\top} + cI \quad (11)$$

236 where $U = [u_1, u_2, \dots, u_k]/\sqrt{k} \in \mathbb{R}^{n \times k}$, $V = [v_1, v_2, \dots, v_k]/\sqrt{k} \in \mathbb{R}^{n \times k}$ and $u_i, v_i \in \mathbb{R}^n$
 237 correspond to the first-order derivatives in Equations (9) and (10), and H_i corresponds to the remaining
 238 terms that involve second-order derivatives. We use a constant identity matrix to approximate H_i ,
 239 while explicitly computing the remaining parts to increase accuracy.

240 However, we still cannot explicitly expand $UV^{\top} \in \mathbb{R}^{n \times n}$ since the dimensionality is too large.
 241 Therefore, we apply Woodbury matrix identity [35] to invert Equation (11):

$$(\nabla_{\pi}^2 J_{\theta}(\pi))^{-1} \approx (UV^{\top} + cI)^{-1} = \frac{1}{c} I - \frac{1}{c} U(cI - V^{\top}U)^{-1} V^{\top} \quad (12)$$

Algorithm 1: Decision-focused Learning for MDP Problems with Missing Parameters

- 1 **Parameter:** Training set $\mathcal{D}_{\text{train}} = \{(x_i, \mathcal{T}_i)\}_{i \in \mathcal{I}_{\text{train}}}$, learning rate α , regularization $\lambda = 0.1$
 - 2 **Initialization:** Initialize predictive model $m_w : \mathcal{X} \rightarrow \Theta$ parameterized by w
 - 3 **for** $\text{epoch} \in \{1, 2, \dots\}$, **each training instance** $(x, \mathcal{T}) \in \mathcal{D}_{\text{train}}$ **do**
 - 4 **Forward:** Make prediction $\theta = m_w(x)$. Compute two-stage loss $\mathcal{L}(\theta, \mathcal{T})$. Run model-free RL to get an optimal policy $\pi^*(\theta)$ on MDP problem using parameter θ .
 - 5 **Backward:** Sample a set of trajectories under θ, π^* to compute $\nabla_{\pi}^2 J_{\theta}(\pi^*), \nabla_{\theta\pi}^2 J_{\theta}(\pi^*)$
 - 6 **Gradient step:** Set $\Delta w = \frac{d \text{Eval}_{\mathcal{T}}(\pi^*)}{dw} - \lambda \frac{d\mathcal{L}(\theta, \mathcal{T})}{dw}$ by Equation (8) with predictive loss \mathcal{L} as regularization. Run gradient ascent to update model: $w \leftarrow w + \alpha \Delta w$
 - 7 **Return:** Predictive model m_w .
-

242 where $V^{\top}U \in \mathbb{R}^{k \times k}$ can be efficiently computed with much smaller $k \ll n$. When we compute
243 the full gradient for decision-focused learning in Equation (8), we can then apply matrix-vector
244 multiplication without expanding the full high-dimensional matrix, which results in a computation
245 cost of $O(nk + k^{\omega})$ that is much smaller than the full computation cost $O(n^2 + n^{\omega})$.

246 The full algorithm for decision-focused learning in MDPs is illustrated in Algorithm 1.

247 7 Example MDP Problems with Missing Parameters

248 **Gridworld with unknown cliffs** We consider a Gridworld environment with a set of training and
249 test MDPs. Each MDP is a 5×5 grid with a start state located at the bottom left corner and a safe
250 state with reward drawn from $\mathcal{N}(5, 1)$ located at the top right corner. Each intermediate state has a
251 reward associated with it, where most of them give the agent a reward drawn from $\mathcal{N}(0, 1)$ but 20%
252 of the them are cliffs and give $\mathcal{N}(-10, 1)$ penalty to the agent. The agent has no prior information
253 about the reward of each grid cell (i.e., the reward functions of the MDPs are unknown), but has
254 a feature vector per grid cell correlated to the reward, and a set of historical trajectories from the
255 training MDPs. The agent learns a predictive model to map from the features of a grid cell to its
256 missing reward information, and the resulting MDP is used to plan. Since the state and action spaces
257 are both finite, we use tabular value-iteration [28] to solve the MDPs.

258 **Partially observable snare-finding problems with missing transition function** We consider a
259 set of *synthetic* conservation parks, each with 20 sites, that are vulnerable to poaching activities. Each
260 site in a conservation park starts from a *safe* state and has an unknown associated probability that a
261 poacher places a snare at each time step. Motivated by [36], we assume a ranger who can visit one
262 site per time step and observes whether a snare is present. If a snare is present, the ranger removes
263 it and receives reward 1. Otherwise, the ranger receives reward of -1 . As the ranger receives no
264 information about the sites that they do not visit, the MDP belief state is the ranger’s belief about
265 whether a snare is present. The ranger uses the features of each site and historical trajectories to learn
266 a predictive model of the missing transition probability of a snare being placed. Since the belief
267 state is continuous and the action space is discrete, given a predictive model of the missing transition
268 probability, the agent uses double deep Q-learning (DDQN) [30] to solve the predicted MDPs.

269 **Partially observable patient treatment problems with missing transition probability** We con-
270 sider a version of the Tuberculosis Adherence Problem explored in [22]. Given that the treatment for
271 tuberculosis requires patients to take medications for an extended period of time, one way to improve
272 patient adherence is Directly Observed Therapy, in which a healthcare worker routinely checks in on
273 the patient to ensure that they are taking their medications. In our problem, we consider 5 *synthetic*
274 patients who have to take medication for 30 days. Each day, a healthcare worker chooses one patient
275 to intervene on. They observe whether that patient is adhering or not, and improve the patient’s
276 likelihood of adhering on that day, where we use the number of adherent patients as the reward to
277 the healthcare worker. Whether a patient actually adheres or not is determined by a transition matrix
278 that is randomly drawn from a fixed distribution inspired by [17]. The aim of the prediction stage is
279 to predict these transition matrices given features associated with each patient. The aim of the RL
280 stage is then to create an intervention strategy for the healthcare worker such that the sum of patient

Table 1: OPE performances of different methods on the test MDPs averaged over 30 independent runs. Decision-focused learning methods consistently outperform two-stage approach, with some exception using identity matrix based Hessian approximation which may lead to high gradient variance.

Trajectories	Gridworld		Snare		Tuberculosis	
	Random	Near-optimal	Random	Near-optimal	Random	Near-optimal
TS	-12.0±1.3	4.2±0.8	0.8±0.3	3.7±0.3	35.8±1.5	38.7±1.6
PG-Id	-11.7±1.2	5.7±0.8	-0.1±0.3	3.6±0.3	38.4±1.5	40.7±1.7
Bellman-Id	-9.7±1.2	4.8±0.7	0.7±0.4	3.6±0.3	39.1±1.7	40.8±1.7
PG-W	-11.2±1.2	5.5±0.8	1.2±0.4	4.8±0.3	38.4±1.5	40.8±1.7
Bellman-W	-10.9±1.2	4.8±0.7	1.5±0.4	4.3±0.3	38.6±1.6	41.1±1.7

281 adherence over the 30-day period is maximised. Due to partial observability, we convert the problem
 282 to its continuous belief state equivalence and solve it using DDQN.

283 Please refer to Appendix C for more details about problem setup in all three domains.

284 8 Experimental Results and Discussion

285 In our experiments, we compare two-stage learning (**TS**) with different versions of decision-focused
 286 learning (**DF**) using two different optimality conditions, policy gradient (**PG**) and Bellman equation-
 287 based (**Bellman**), and two different Hessian approximations (**Identity**, **Woodbury**) defined in Sec-
 288 tion 6. Computing the **full** Hessian (as in Section 6.1) is computationally intractable. Across all three
 289 examples, we use 7 training MDPs, 1 validation MDP, and 2 test MDPs, each with 100 trajectories.
 290 The predictive model is trained on the training MDP trajectories for 100 epochs. Performance is evalu-
 291 ated under the Off-Policy Evaluation (OPE) metric of Equation (1) with respect to the withheld test
 292 trajectories. In the following, we will discuss *how* DF variants work compared with TS methods, and
 293 explore *why* some methods are better. We use two different trajectories, **random** and **near-optimal**,
 294 in the training MDP to model different imbalanced information given to train the predictive model.
 295 The results are shown in Table 1.

296 **Decision-focused learning with the Woodbury matrix identity outperforms two-stage learning**
 297 Table 1 summarizes the average OPE performance on the test MDPs. We can see that in all of the
 298 three problem settings, the best performances are all achieved by decision-focused learning. However,
 299 when Hessian approximation is not sufficiently accurate, decision-focused learning can sometimes
 300 perform even worse than two-stage (e.g., PG-Id and Bellman-Id in the snare problem). In contrast,
 301 decision-focused methods using a more accurate low-rank approximation and Woodbury matrix
 302 identity (i.e., PG-W and Bellman-W), as discussed in Section 6.3, dominate two-stage performance
 303 in the test MDPs across all settings.

304 **Low predictive loss does not imply a winning policy** In Figures 2(a), 3(a), we plot the predictive
 305 loss curve in the training MDPs over different training epochs of Gridworld and snare problems. In
 306 particular, two-stage approach is trained to minimize such loss, but fails to win in Table 1. Indeed, low
 307 predictive loss on the training MDPs does not always imply a high off-policy evaluation on the training
 308 MDPs in Figure 2(b) due to the misalignment of predictive accuracy and decision quality, which is
 309 consistent with other studies in mismatch of predictive loss and evaluation metric [5, 13, 14, 19].

310 **Comparison between different Hessian approximations** In Table 1, we notice that more inaccur-
 311 ate Hessian approximation (identity) does not always lead to poorer performance. We hypothesize
 312 that this is due to the non-convex off-policy evaluation objective that we are optimizing, where higher
 313 variance might sometimes help escape local optimum more easily. The identity approximation is
 314 more unstable across different tasks and different trajectories given. In Table 1, the performance of
 315 Bellman-Identity and PG-Identity sometimes lead to wins over two stage and sometimes losses.

316 **Comparison between policy gradient and Bellman-based decision-focused learning** We ob-
 317 serve that the Bellman-based decision-focused approach consistently outperforms the policy gradient-
 318 based approach when the trajectories are random, while the policy gradient-based decision-focused

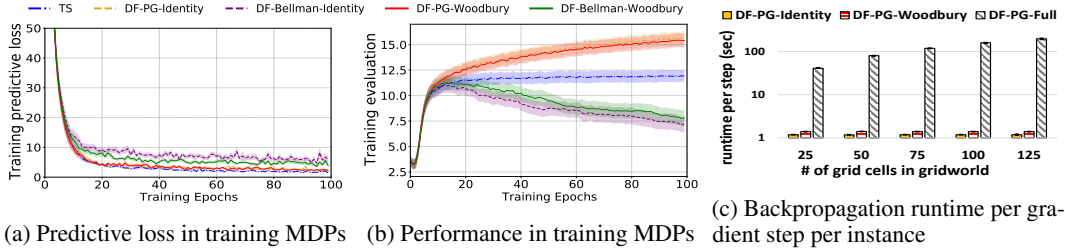


Figure 2: Learning curves of Gridworld problem with near-optimal trajectories. Two-stage minimizes the predictive loss in Figure 2(a), but this does not lead to good training performance in Figure 2(b). Figure 3(c) shows the backpropagation runtime per gradient step per instance of three Hessian approximations, which becomes intractable when trained for multiple instances and multiple epochs.

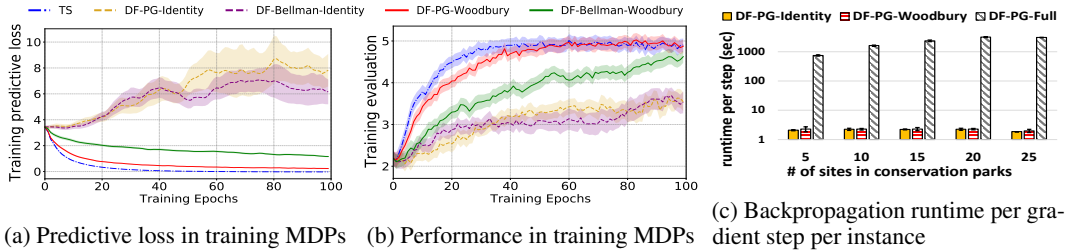


Figure 3: Learning curves of snare finding problems with random trajectories. Two-stage achieves both low predictive loss in Figure 3(a) and high training OPE in Figure 3(b), but the test performance is poor in Table 1. Figure 3(c) plots the backpropagation runtime per gradient step per instance.

319 approach mostly achieves better performance when near-optimal trajectories are present. We hy-
 320 pothesize that this is due to the different objectives considered by different optimality conditions.
 321 The Bellman error aims to accurately cover *all* the value functions, which works better on random
 322 trajectories; the policy gradient aims to maximize the expected cumulative reward along the *optimal*
 323 *policy only*, which works better with near-optimal trajectories that have better coverage in the optimal
 324 regions.

325 **Computation cost** Lastly, Figures 2(c) and 3(c) show the backpropagation runtime of the policy-
 326 gradient based optimality condition per gradient step per training instance across different Hessian
 327 approximations and different problem sizes in the gridworld and snare finding problems. To train
 328 the model, we run 100 epochs for every MDP in the training set, which immediately makes the full
 329 Hessian computation intractable as it would take more than a day to complete.

330 Analytically, let n be the dimensionality of the policy space and $k \ll n$ be the number of sampled
 331 trajectories used to approximate the derivatives. As shown in Section 6, the computation cost of full
 332 Hessian $O(n^2 + n^\omega)$ is quadratic in n and strictly dominates all the others. In contrast, the costs of
 333 the identity matrix approximation $O(nk)$ and the Woodbury approximation $O(nk + k^\omega)$ are both
 334 linear in n . The Woodbury method offers an option to get a more accurate Hessian at low additional
 335 cost.

336 9 Conclusion

337 This paper considers learning a predictive model to address the missing parameters in sequential
 338 decision problems. We successfully extend decision-focused learning from optimization problems to
 339 MDP problems solved by deep reinforcement learning algorithms, where we apply sampling and
 340 low-rank approximation to Hessian matrix computation to address the associated computational
 341 challenges. All our results suggest that decision-focused learning can outperform two-stage approach
 342 by directly optimizing the final evaluation metric. The idea of considering sequential decision
 343 problems as differentiable layers also suggests a different way to solve online reinforcement learning
 344 problems, which we reserve as a future direction.

References

- 345
- 346 [1] A. Agrawal, B. Amos, S. Barratt, S. Boyd, S. Diamond, and Z. Kolter. Differentiable convex
347 optimization layers. *arXiv preprint arXiv:1910.12430*, 2019.
- 348 [2] B. Amos, I. D. J. Rodriguez, J. Sacks, B. Boots, and J. Z. Kolter. Differentiable mpc for
349 end-to-end planning and control. *arXiv preprint arXiv:1810.13400*, 2018.
- 350 [3] S. Bai, J. Z. Kolter, and V. Koltun. Deep equilibrium models. *arXiv preprint arXiv:1909.01377*,
351 2019.
- 352 [4] O. E. Balghithi, A. N. Elmachtoub, P. Grigas, and A. Tewari. Generalization bounds in the
353 predict-then-optimize framework. *arXiv preprint arXiv:1905.11488*, 2019.
- 354 [5] P. Branco, L. Torgo, and R. P. Ribeiro. A survey of predictive modeling on imbalanced domains.
355 *ACM Computing Surveys (CSUR)*, 49(2):1–50, 2016.
- 356 [6] P. L. Donti, B. Amos, and J. Z. Kolter. Task-based end-to-end model learning in stochastic
357 optimization. *arXiv preprint arXiv:1703.04529*, 2017.
- 358 [7] Y. Duan, J. Schulman, X. Chen, P. L. Bartlett, I. Sutskever, and P. Abbeel. Rl^2 : Fast reinforce-
359 ment learning via slow reinforcement learning. *arXiv preprint arXiv:1611.02779*, 2016.
- 360 [8] A. N. Elmachtoub and P. Grigas. Smart “predict, then optimize”. *Management Science*, 2021.
- 361 [9] C. Finn, P. Abbeel, and S. Levine. Model-agnostic meta-learning for fast adaptation of deep
362 networks. In *International Conference on Machine Learning*, pages 1126–1135. PMLR, 2017.
- 363 [10] J. Futoma, M. C. Hughes, and F. Doshi-Velez. Popcorn: Partially observed prediction con-
364 strained reinforcement learning. *arXiv preprint arXiv:2001.04032*, 2020.
- 365 [11] T. Haarnoja, H. Tang, P. Abbeel, and S. Levine. Reinforcement learning with deep energy-based
366 policies. In *International Conference on Machine Learning*, pages 1352–1361. PMLR, 2017.
- 367 [12] T. Haarnoja, A. Zhou, P. Abbeel, and S. Levine. Soft actor-critic: Off-policy maximum entropy
368 deep reinforcement learning with a stochastic actor. In *International Conference on Machine
369 Learning*, pages 1861–1870. PMLR, 2018.
- 370 [13] C. Huang, S. Zhai, W. Talbott, M. B. Martin, S.-Y. Sun, C. Guestrin, and J. Susskind. Addressing
371 the loss-metric mismatch with adaptive loss alignment. In *International Conference on Machine
372 Learning*, pages 2891–2900. PMLR, 2019.
- 373 [14] J. M. Johnson and T. M. Khoshgoftaar. Survey on deep learning with class imbalance. *Journal
374 of Big Data*, 6(1):1–54, 2019.
- 375 [15] P. Karkus, X. Ma, D. Hsu, L. P. Kaelbling, W. S. Lee, and T. Lozano-Pérez. Differentiable
376 algorithm networks for composable robot learning. *arXiv preprint arXiv:1905.11602*, 2019.
- 377 [16] R. Kidambi, A. Rajeswaran, P. Netrapalli, and T. Joachims. Morel: Model-based offline
378 reinforcement learning. *arXiv preprint arXiv:2005.05951*, 2020.
- 379 [17] J. A. Killian, B. Wilder, A. Sharma, V. Choudhary, B. Dilkina, and M. Tambe. Learning to
380 prescribe interventions for tuberculosis patients using digital adherence data. In *Proceedings of
381 the 25th ACM SIGKDD International Conference on Knowledge Discovery & Data Mining*,
382 pages 2430–2438, 2019.
- 383 [18] P. R. Kumar and P. Varaiya. *Stochastic systems: Estimation, identification, and adaptive control*.
384 SIAM, 2015.
- 385 [19] N. Lambert, B. Amos, O. Yadan, and R. Calandra. Objective mismatch in model-based
386 reinforcement learning. *arXiv preprint arXiv:2002.04523*, 2020.
- 387 [20] A. Lazaric. Transfer in reinforcement learning: a framework and a survey. In *Reinforcement
388 Learning*, pages 143–173. Springer, 2012.

- 389 [21] J. Mandi and T. Guns. Interior point solving for lp-based prediction+ optimisation. *arXiv preprint arXiv:2010.13943*, 2020.
390
- 391 [22] A. Mate, J. A. Killian, H. Xu, A. Perrault, and M. Tambe. Collapsing bandits and their
392 application to public health interventions. *arXiv preprint arXiv:2007.04432*, 2020.
- 393 [23] A. Y. Ng, D. Harada, and S. Russell. Policy invariance under reward transformations: Theory
394 and application to reward shaping. In *Icml*, volume 99, pages 278–287, 1999.
- 395 [24] C. Ning and F. You. Optimization under uncertainty in the era of big data and deep learning:
396 When machine learning meets mathematical programming. *Computers & Chemical Engineering*,
397 125:434–448, 2019.
- 398 [25] A. Perrault, B. Wilder, E. Ewing, A. Mate, B. Dilkina, and M. Tambe. End-to-end game-focused
399 learning of adversary behavior in security games. In *Proceedings of the AAAI Conference on*
400 *Artificial Intelligence*, volume 34, pages 1378–1386, 2020.
- 401 [26] N. V. Sahinidis. Optimization under uncertainty: state-of-the-art and opportunities. *Computers*
402 *& Chemical Engineering*, 28(6-7):971–983, 2004.
- 403 [27] T. Schaul, D. Horgan, K. Gregor, and D. Silver. Universal value function approximators. In
404 *International conference on machine learning*, pages 1312–1320. PMLR, 2015.
- 405 [28] R. S. Sutton. Integrated architectures for learning, planning, and reacting based on approximating
406 dynamic programming. In *Machine learning proceedings 1990*, pages 216–224. Elsevier, 1990.
- 407 [29] M. E. Taylor and P. Stone. Transfer learning for reinforcement learning domains: A survey.
408 *Journal of Machine Learning Research*, 10(7), 2009.
- 409 [30] H. Van Hasselt, A. Guez, and D. Silver. Deep reinforcement learning with double q-learning.
410 In *AAAI*, 2016.
- 411 [31] J. X. Wang, Z. Kurth-Nelson, D. Tirumala, H. Soyer, J. Z. Leibo, R. Munos, C. Blundell, D. Ku-
412 maran, and M. Botvinick. Learning to reinforcement learn. *arXiv preprint arXiv:1611.05763*,
413 2016.
- 414 [32] K. Wang, B. Wilder, A. Perrault, and M. Tambe. Automatically learning compact quality-aware
415 surrogates for optimization problems. *arXiv preprint arXiv:2006.10815*, 2020.
- 416 [33] Y. Wang, Y. Ge, L. Li, R. Chen, and T. Xu. Offline meta-level model-based reinforcement
417 learning approach for cold-start recommendation. *arXiv preprint arXiv:2012.02476*, 2020.
- 418 [34] B. Wilder, B. Dilkina, and M. Tambe. Melding the data-decisions pipeline: Decision-focused
419 learning for combinatorial optimization. In *Proceedings of the AAAI Conference on Artificial*
420 *Intelligence*, volume 33, pages 1658–1665, 2019.
- 421 [35] M. A. Woodbury. *Inverting modified matrices*. Statistical Research Group, 1950.
- 422 [36] L. Xu, S. Gholami, S. Mc Carthy, B. Dilkina, A. Plumtre, M. Tambe, R. Singh, M. Nsubuga,
423 J. Mabonga, M. Driciru, et al. Stay ahead of poachers: Illegal wildlife poaching prediction and
424 patrol planning under uncertainty with field test evaluations (short version). In *2020 IEEE 36th*
425 *International Conference on Data Engineering (ICDE)*, pages 1898–1901. IEEE, 2020.
- 426 [37] T. Yu, A. Kumar, R. Rafailov, A. Rajeswaran, S. Levine, and C. Finn. Combo: Conservative
427 offline model-based policy optimization. *arXiv preprint arXiv:2102.08363*, 2021.
- 428 [38] L. Zintgraf, K. Shiarlis, M. Igl, S. Schulze, Y. Gal, K. Hofmann, and S. Whiteson. Varibad: A
429 very good method for bayes-adaptive deep rl via meta-learning. In *International Conference on*
430 *Learning Representations*, 2019.

431 **Checklist**

- 432 1. For all authors...
- 433 (a) Do the main claims made in the abstract and introduction accurately reflect the paper's
434 contributions and scope? [Yes]
- 435 (b) Did you describe the limitations of your work? [Yes] Please refer to Appendix B
- 436 (c) Did you discuss any potential negative societal impacts of your work? [N/A]
- 437 (d) Have you read the ethics review guidelines and ensured that your paper conforms to
438 them? [Yes]
- 439 2. If you are including theoretical results...
- 440 (a) Did you state the full set of assumptions of all theoretical results? [Yes]
- 441 (b) Did you include complete proofs of all theoretical results? [Yes] Please refer to
442 Appendix A
- 443 3. If you ran experiments...
- 444 (a) Did you include the code, data, and instructions needed to reproduce the main experi-
445 mental results (either in the supplemental material or as a URL)? [Yes] Please refer to
446 the supplementary material
- 447 (b) Did you specify all the training details (e.g., data splits, hyperparameters, how they
448 were chosen)? [Yes] Please refer to Appendix C
- 449 (c) Did you report error bars (e.g., with respect to the random seed after running experi-
450 ments multiple times)? [Yes]
- 451 (d) Did you include the total amount of compute and the type of resources used (e.g., type
452 of GPUs, internal cluster, or cloud provider)? [Yes] Please refer to Appendix E
- 453 4. If you are using existing assets (e.g., code, data, models) or curating/releasing new assets...
- 454 (a) If your work uses existing assets, did you cite the creators? [Yes] All data are synthetic
455 except for the transition probabilities used to generate synthetic patients are taken
456 from [17], and we provide reference to the papers that inspired them.
- 457 (b) Did you mention the license of the assets? [N/A]
- 458 (c) Did you include any new assets either in the supplemental material or as a URL? [N/A]
- 459
- 460 (d) Did you discuss whether and how consent was obtained from people whose data you're
461 using/curating? [N/A]
- 462 (e) Did you discuss whether the data you are using/curating contains personally identifiable
463 information or offensive content? [N/A]
- 464 5. If you used crowdsourcing or conducted research with human subjects...
- 465 (a) Did you include the full text of instructions given to participants and screenshots, if
466 applicable? [N/A]
- 467 (b) Did you describe any potential participant risks, with links to Institutional Review
468 Board (IRB) approvals, if applicable? [N/A]
- 469 (c) Did you include the estimated hourly wage paid to participants and the total amount
470 spent on participant compensation? [N/A]

471 **Appendix**

472 **A Proofs**

473 **Theorem 1** (Policy gradient-based unbiased derivative estimate). *We follow the notation of Defini-*
 474 *tion 1 and define $\Phi_\theta(\tau, \pi) = \sum_{i=1}^h \sum_{j=i}^h \gamma^j R_\theta(s_j, a_j) \log \pi(a_i | s_i)$. We have:*

$$\nabla_\pi J_\theta(\pi) = \mathbb{E}_{\tau \sim \pi, \theta} [\nabla_\pi \Phi_\theta(\tau, \pi)] \implies \begin{aligned} \nabla_\pi^2 J_\theta(\pi) &= \mathbb{E}_{\tau \sim \pi, \theta} [\nabla_\pi \Phi_\theta \cdot \nabla_\pi \log p_\theta^\top + \nabla_\pi^2 \Phi_\theta] \\ \nabla_{\theta\pi}^2 J_\theta(\pi) &= \mathbb{E}_{\tau \sim \pi, \theta} [\nabla_\pi \Phi_\theta \cdot \nabla_\theta \log p_\theta^\top + \nabla_{\theta\pi}^2 \Phi_\theta] \end{aligned} \quad (9)$$

475 *First part of the proof (policy gradient theorem).* The first part of the proof follows the policy gradi-
 476 *ent theorem. We begin with definitions.*

477 Let $\tau = \{s_1, a_1, s_2, a_2, \dots, s_h, a_h\}$ be a trajectory sampled according to policy π and MDP param-
 478 *eter θ . Define $\tau_j = \{s_1, a_1, \dots, s_j, a_j\}$ to be a partial trajectory up to time step j for any $j \in [h]$.*

479 *Define $G_\theta(\tau) = \sum_{j=1}^h \gamma^j R_\theta(s_j, a_j)$ to be the discounted value of trajectory τ . Let $p_\theta(\tau, \pi)$ be the*
 480 *probability of seeing trajectory τ under parameter θ and policy π . Given MDP parameter θ , we can*
 481 *compute the expected cumulative reward of policy π by:*

$$\begin{aligned} J_\theta(\pi) &= \mathbf{E}_{\tau \sim \pi, \theta} G_\theta(\tau) \\ &= \mathbf{E}_{\tau \sim \pi, \theta} \sum_{j=1}^h \gamma^j R_\theta(s_j, a_j) \\ &= \sum_{j=1}^h \mathbf{E}_{\tau \sim p_\theta(\tau, \pi)} \gamma^j R_\theta(s_j, a_j) \end{aligned} \quad (13)$$

$$\begin{aligned} &= \sum_{j=1}^h \mathbf{E}_{\tau_j \sim p_\theta(\tau_j, \pi)} \gamma^j R_\theta(s_j, a_j) \\ &= \sum_{j=1}^h \int_{\tau_j} \gamma^j R_\theta(s_j, a_j) p_\theta(\tau_j, \pi) d\tau_j \end{aligned} \quad (14)$$

482 Equation 13 to Equation 14 uses the fact that we only need to sample up to time step j in order to
 483 compute $\gamma^j R_\theta(s_j, a_j)$. Everything beyond time step j does not affect the expectation up to time step
 484 j . We can compute the policy gradient by:

$$\begin{aligned} \nabla_\pi J_\theta(\pi) &= \nabla_\pi \sum_{j=1}^h \int_{\tau_j} \gamma^j R_\theta(s_j, a_j) p_\theta(\tau_j, \pi) d\tau_j \\ &= \sum_{j=1}^h \int_{\tau_j} \gamma^j R_\theta(s_j, a_j) \nabla_\pi p_\theta(\tau_j, \pi) d\tau_j \end{aligned} \quad (15)$$

$$= \sum_{j=1}^h \int_{\tau_j} \gamma^j R_\theta(s_j, a_j) p_\theta(\tau_j, \pi) \nabla_\pi \log p_\theta(\tau_j, \pi) d\tau_j \quad (16)$$

485 where Equation 15 is because only the probability term is dependent on policy π , and Equation 16 is
 486 by $\nabla_\pi p_\theta = p_\theta \nabla_\pi \log p_\theta$.

487 We can now merge the integral back to an expectation over trajectory τ_j by merging the probability
 488 term p_θ and the integral:

$$\begin{aligned}
 \nabla_\pi J_\theta(\pi) &= \sum_{j=1}^h \mathbf{E}_{\tau_j \sim p_\theta(\tau_j, \pi)} [\gamma^j R_\theta(s_j, a_j) \nabla_\pi \log p_\theta(\tau_j, \pi)] \\
 &= \sum_{j=1}^h \mathbf{E}_{\tau \sim p_\theta(\tau, \pi)} [\gamma^j R_\theta(s_j, a_j) \nabla_\pi \log p_\theta(\tau_j, \pi)] \\
 &= \mathbf{E}_{\tau \sim p_\theta(\tau, \pi)} \left[\sum_{j=1}^h \gamma^j R_\theta(s_j, a_j) \nabla_\pi \log p_\theta(\tau_j, \pi) \right] \\
 &= \mathbf{E}_{\tau \sim p_\theta(\tau, \pi)} \left[\sum_{j=1}^h \gamma^j R_\theta(s_j, a_j) \nabla_\pi \left(\sum_{i=1}^j \log \pi(a_i | s_i) + \sum_{i=1}^j \log p_\theta(s_i, a_i, s_{i+1}) \right) \right] \\
 & \tag{17} \\
 &= \mathbf{E}_{\tau \sim p_\theta(\tau, \pi)} \left[\sum_{j=1}^h \gamma^j R_\theta(s_j, a_j) \sum_{i=1}^j \nabla_\pi \log \pi(a_i | s_i) \right] \\
 &= \mathbf{E}_{\tau \sim p_\theta(\tau, \pi)} \left[\sum_{j=1}^h \sum_{i=1}^j \gamma^j R_\theta(s_j, a_j) \nabla_\pi \log \pi(a_i | s_i) \right] \\
 &= \mathbf{E}_{\tau \sim p_\theta(\tau, \pi)} \left[\sum_{i=1}^h \sum_{j=i}^h \gamma^j R_\theta(s_j, a_j) \nabla_\pi \log \pi(a_i | s_i) \right] \\
 &= \mathbf{E}_{\tau \sim p_\theta(\tau, \pi)} [\nabla_\pi \Phi_\theta(\tau, \pi)] \tag{18}
 \end{aligned}$$

489 where Equation 17 is by expanding the probability of seeing trajectory τ_j when parameter θ and
 490 policy π are used, where the probability decomposes into the first term action probability $\pi(a_i | s_i)$,
 491 and the second term transition probability $p_\theta(s_i, a_i, s_{i+1})$, which is independent of policy π and thus
 492 disappears. The last equation in Equation 18 connects back to the definition of Φ as defined in the
 493 statement of Theorem 1. Φ is easy to compute and easy to differentiate through. We can therefore
 494 sample a set of trajectories $\{\tau\}$ to compute the corresponding Φ and its derivative to get the unbiased
 495 policy gradient estimate. \square

496 *Second part of the proof (second-order derivatives).* Given the policy gradient theorem as we recall
 497 in the above derivation, we have:

$$\nabla_\pi J_\theta(\pi) = \mathbf{E}_{\tau \sim p_\theta(\tau, \pi)} [\nabla_\pi \Phi_\theta(\tau, \pi)] \tag{19}$$

498 We can compute the derivative of Equation 19 by:

$$\begin{aligned}
 \nabla_\pi^2 J_\theta(\pi) &= \nabla_\pi \nabla_\pi J_\theta(\pi) \\
 &= \nabla_\pi \mathbf{E}_{\tau \sim p_\theta(\tau, \pi)} [\nabla_\pi \Phi_\theta(\tau, \pi)] \\
 &= \nabla_\pi \int_\tau \nabla_\pi \Phi_\theta(\tau, \pi) p_\theta(\tau, \pi) d\tau \\
 &= \int_\tau [\nabla_\pi \Phi_\theta(\tau, \pi) \nabla_\pi p_\theta(\tau, \pi)^\top + \nabla_\pi^2 \Phi_\theta(\tau, \pi) p_\theta(\tau, \pi)] d\tau \tag{20}
 \end{aligned}$$

$$\begin{aligned}
 &= \int_\tau [\nabla_\pi \Phi_\theta(\tau, \pi) \nabla_\pi \log p_\theta(\tau, \pi)^\top + \nabla_\pi^2 \Phi_\theta(\tau, \pi)] p_\theta(\tau, \pi) d\tau \\
 &= \mathbf{E}_{\tau \sim p_\theta(\tau, \pi)} [\nabla_\pi \Phi_\theta(\tau, \pi) \nabla_\pi \log p_\theta(\tau, \pi)^\top + \nabla_\pi^2 \Phi_\theta(\tau, \pi)] \tag{21}
 \end{aligned}$$

499 where Equation 20 passes gradient inside the integral and applies chain rule. Equation 21 provides an
 500 unbiased estimate of the second-order derivative $\nabla_\pi^2 J_\theta(\pi)$.

501 Similarly, we can compute:

$$\begin{aligned}
\nabla_{\theta\pi}^2 J_\theta(\pi) &= \nabla_\theta \nabla_\pi J_\theta(\pi) \\
&= \nabla_\theta \mathbf{E}_{\tau \sim p_\theta(\tau, \pi)} [\nabla_\pi \Phi_\theta(\tau, \pi)] \\
&= \nabla_\theta \int_\tau \nabla_\pi \Phi_\theta(\tau, \pi) p_\theta(\tau, \pi) d\tau \\
&= \int_\tau [\nabla_\pi \Phi_\theta(\tau, \pi) \nabla_\theta p_\theta(\tau, \pi)^\top + \nabla_{\theta\pi}^2 \Phi_\theta(\tau, \pi) p_\theta(\tau, \pi)] d\tau \\
&= \int_\tau [\nabla_\pi \Phi_\theta(\tau, \pi) \nabla_\theta \log p_\theta(\tau, \pi)^\top + \nabla_{\theta\pi}^2 \Phi_\theta(\tau, \pi)] p_\theta(\tau, \pi) d\tau \\
&= \mathbf{E}_{\tau \sim p_\theta(\tau, \pi)} [\nabla_\pi \Phi_\theta(\tau, \pi) \nabla_\theta \log p_\theta(\tau, \pi)^\top + \nabla_{\theta\pi}^2 \Phi_\theta(\tau, \pi)] \quad (22)
\end{aligned}$$

502 Equation 21 and Equation 22 both serve as unbiased estimates of the corresponding second-order
503 derivatives. We can sample a set of trajectories to compute both of them and get an unbiased estimate
504 of the second-order derivatives. This concludes the proof of Theorem 1. \square

505 **Theorem 2** (Bellman-based unbiased derivative estimate). *We follow the notation in Definition 2 to*
506 *define $J_\theta(\pi) = \frac{1}{2} \mathbf{E}_{\tau \sim \pi, \theta} [\delta_\theta^2(\tau, \pi)]$. We have:*

$$\begin{aligned}
\nabla_\pi J_\theta(\pi) &= \mathbf{E}_{\tau \sim \pi, \theta} \left[\delta \nabla_\pi \delta + \frac{1}{2} \delta^2 \nabla_\pi \log p_\theta \right] \implies \nabla_\pi^2 J_\theta(\pi) = \mathbf{E}_{\tau \sim \pi, \theta} [\nabla_\pi \delta \nabla_\pi \delta^\top + O(\delta)] \\
\nabla_{\theta\pi}^2 J_\theta(\pi) &= \mathbf{E}_{\tau \sim \pi, \theta} [\nabla_\pi \delta \nabla_\theta \delta^\top + (\nabla_\pi \delta \nabla_\theta \log p_\theta^\top + \nabla_\pi \log p_\theta \nabla_\theta \delta^\top + \nabla_{\theta\pi}^2 \delta) \delta + O(\delta^2)] \quad (10)
\end{aligned}$$

507 *First part of the proof (first-order derivative).* By the definition of $J_\theta(\pi) = \frac{1}{2} \mathbf{E}_{\tau \sim \pi, \theta} [\delta^2(\tau, \pi)]$,
508 we can compute its first-order derivative by:

$$\begin{aligned}
\nabla_\pi J_\theta(\pi) &= \nabla_\pi \frac{1}{2} \mathbf{E}_{\tau \sim \pi, \theta} [\delta_\theta^2(\tau, \pi)] \\
&= \nabla_\pi \frac{1}{2} \int_\tau \delta_\theta^2(\tau, \pi) p_\theta(\tau, \pi) d\tau \\
&= \int_\tau \left[p_\theta(\tau, \pi) \delta_\theta(\tau, \pi) \nabla_\pi \delta_\theta(\tau, \pi) + \frac{1}{2} \delta_\theta^2(\tau, \pi) \nabla_\pi p_\theta(\tau, \pi) \right] d\tau \\
&= \int_\tau \left[\delta_\theta(\tau, \pi) \nabla_\pi \delta_\theta(\tau, \pi) + \frac{1}{2} \delta_\theta^2(\tau, \pi) \nabla_\pi \log p_\theta(\tau, \pi) \right] p_\theta(\tau, \pi) d\tau \\
&= \mathbf{E}_{\tau \sim \pi, \theta} \left[\delta_\theta(\tau, \pi) \nabla_\pi \delta_\theta(\tau, \pi) + \frac{1}{2} \delta_\theta^2(\tau, \pi) \nabla_\pi \log p_\theta(\tau, \pi) \right] \quad (23)
\end{aligned}$$

509 \square

510 *Second part of the proof (second-order derivative).* Given Equation 23, we can further compute the
511 second-order derivatives by:

$$\begin{aligned}
\nabla_\pi^2 J_\theta(\pi) &= \nabla_\pi \nabla_\pi J_\theta(\pi) \\
&= \nabla_\pi \mathbf{E}_{\tau \sim \pi, \theta} \left[\delta_\theta(\tau, \pi) \nabla_\pi \delta_\theta(\tau, \pi) + \frac{1}{2} \delta_\theta^2(\tau, \pi) \nabla_\pi \log p_\theta(\tau, \pi) \right] \\
&= \nabla_\pi \int_\tau \left[\delta_\theta(\tau, \pi) \nabla_\pi \delta_\theta(\tau, \pi) + \frac{1}{2} \delta_\theta^2(\tau, \pi) \nabla_\pi \log p_\theta(\tau, \pi) \right] p_\theta(\tau, \pi) d\tau \\
&= \int_\tau \left(\nabla_\pi \delta \nabla_\pi \delta^\top + \delta \nabla_\pi^2 \delta + \delta \nabla \log p_\theta \nabla_\pi \delta^\top + \frac{1}{2} \delta^2 \nabla^2 \log p_\theta \right) p_\theta \\
&\quad + \left(\delta \nabla_\pi \delta(\tau, \pi) + \frac{1}{2} \delta^2 \nabla_\pi \log p_\theta \right) p_\theta \nabla \log p_\theta^\top d\tau \\
&= \mathbf{E}_{\tau \sim \pi, \theta} [\nabla_\pi \delta \nabla_\pi \delta^\top + \delta \nabla_\pi^2 \delta + \delta \nabla \log p_\theta \nabla_\pi \delta^\top + \delta \nabla_\pi \delta(\tau, \pi) \nabla \log p_\theta^\top + O(\delta^2)] \\
&= \mathbf{E}_{\tau \sim \pi, \theta} [\nabla_\pi \delta \nabla_\pi \delta^\top + O(\delta)]
\end{aligned}$$

512 Similarly, we have:

$$\begin{aligned}
\nabla_{\theta\pi}^2 J_{\theta}(\pi) &= \nabla_{\theta} \nabla_{\pi} J_{\theta}(\pi) \\
&= \nabla_{\theta} \mathbf{E}_{\tau \sim \pi, \theta} \left[\delta_{\theta}(\tau, \pi) \nabla_{\pi} \delta_{\theta}(\tau, \pi) + \frac{1}{2} \delta_{\theta}^2(\tau, \pi) \nabla_{\pi} \log p_{\theta}(\tau, \pi) \right] \\
&= \nabla_{\theta} \int_{\tau} \left[\delta_{\theta} \nabla_{\pi} \delta_{\theta} + \frac{1}{2} \delta_{\theta}^2 \nabla_{\pi} \log p_{\theta} \right] p_{\theta} d\tau \\
&= \int_{\tau} \left(\nabla_{\pi} \delta \nabla_{\theta} \delta^{\top} + \delta \nabla_{\theta\pi}^2 \delta + \delta \nabla_{\pi} \log p_{\theta} \nabla_{\theta} \delta^{\top} + \frac{1}{2} \delta^2 \nabla_{\theta\pi}^2 \log p_{\theta} \right) p_{\theta} \\
&\quad + \left(\delta \nabla_{\pi} \delta + \frac{1}{2} \delta^2 \nabla_{\pi} \log p_{\theta} \right) p_{\theta} \nabla_{\theta} \log p_{\theta}^{\top} d\tau \\
&= \mathbf{E}_{\tau \sim \pi, \theta} \left[\nabla_{\pi} \delta \nabla_{\theta} \delta^{\top} + \delta \nabla_{\theta\pi}^2 \delta + \delta \nabla_{\pi} \log p_{\theta} \nabla_{\theta} \delta^{\top} + \delta \nabla_{\pi} \delta \nabla_{\theta} \log p_{\theta}^{\top} + O(\delta^2) \right] \\
&= \mathbf{E}_{\tau \sim \pi, \theta} \left[\nabla_{\pi} \delta \nabla_{\theta} \delta^{\top} + \left(\nabla_{\theta\pi}^2 \delta + \nabla_{\pi} \log p_{\theta} \nabla_{\theta} \delta^{\top} + \nabla_{\pi} \delta \nabla_{\theta} \log p_{\theta}^{\top} \right) \delta + O(\delta^2) \right]
\end{aligned} \tag{24}$$

513 which concludes the proof. \square

514 B Challenges and Limitations of Decision-focused Learning

515 In this section, we summarize some challenges and limitations of applying decision-focused learning
516 to MDPs problems.

517 B.1 Smoothness of the Optimal Policy Derived From Reinforcement Learning Solver

518 In Equation 8, we compute the gradient of the final evaluation metric with respect to the predictive
519 model by applying chain rule. This implicitly requires each individual component in the chain rule to
520 be well-defined. In particular, in Equation 8, we need the derivative of the optimal policy π^* with
521 respect to the MDP parameters θ to be well-defined and non-zero, i.e., the optimal policy needs to be
522 changing smoothly when the input MDP parameters change. This requirement may not be satisfied
523 when the optimal policy is deterministic. For example, any policy induced by Q-learning algorithm
524 using non-smooth argmax operators does not satisfy our requirement. We need to relax all the strict
525 operators in the policy in order to make the whole process smooth.

526 The requirement of having a smooth policy is essentially the same idea of soft Q-learning [11] and
527 soft actor-critic [12] proposed by Haarnoja et al. Soft Q-learning relaxes the Bellman equation to
528 a soft Bellman equation to make the policy smoother, while soft actor-critic adds an entropy term
529 as regularization to make the optimal policy smoother. These relaxed policy not only can make the
530 training smoother as stated in the above papers, but also can allow back-propagation through the
531 optimal policy to the input MDP parameters in our paper. These benefits are all due to the smoothness
532 of the optimal policy. Similar issues arise in decision-focused learning in discrete optimization, with
533 Wilder et al. [34] proposing to relaxing the optimal solution by adding a regularization term, which
534 serves as the same purpose as we relax our optimal policy in the sequential decision problem setting.

535 B.2 Unbiased Second-order Derivative Estimates

536 As we discuss in Section 6, correctly approximating the second-order derivatives is the crux of our
537 algorithm. Incorrect approximation may lead to incorrect gradient direction, which can further lead to
538 divergence. Since the second-order derivative formulation as stated in Theorem 1 and Theorem 2 are
539 both unbiased derivative estimate. However, their accuracy depends on how many samples we use to
540 approximate the derivatives. In our experiments, we use 100 sampled trajectories to approximate the
541 second-order derivatives across three domains. The number of samples required to get a sufficiently
542 accurate derivative estimate may depend on the problem size. Larger problems may require more
543 samples to get a good derivative estimate, but more samples also implies more computation cost
544 required to run the back-propagation.

545 In practice, we find that normalization effect of the Hessian term as discussed in Section 6 is very
546 important to reduce the variance caused by the incorrect derivative estimate. Additionally, we also

547 notice that adding a small additional predictive loss term to run back-propagation can stabilize the
548 training process because the predictive loss does not suffer from sampling variance. This is why we
549 add a weighted predictive loss to the back-propagation in Algorithm 1.

550 C Experimental Setup

551 In this section, we describe how we randomly generate the MDP problems and the corresponding
552 missing parameters.

553 **Feature generation** Across all three domains, once the missing parameters are generated, we feed
554 each MDP parameter into a randomly initialized neural network with two intermediate layers each
555 with 64 neurons, and an output dimension size 16 to generate a feature vector of size 16 for the
556 corresponding MDP parameter. For example, in the gridworld example, each grid cell comes with a
557 missing reward. So the feature corresponding to this grid cell and the missing reward is generated by
558 feeding the missing reward into a randomly initialized neural network to generate a feature vector of
559 size 16 for this particular grid cell. We repeat the same process for all the parameters in the MDP
560 problem, e.g., all the grid cells in the gridworld problem. The randomly initiated neural network
561 uses ReLU layers as nonlinearity followed by a linear layer in the end. The generated features are
562 normalized to mean 0 and variance 1, and we add Gaussian noise $\mathcal{N}(0, 1)$ to the features, with a signal
563 noise ratio is 1 : 3, to model that the original missing parameters may not be perfectly recovered from
564 the noisy features. The predictive model we use to map from generated noisy features to the missing
565 parameters is a single layer neural network with 16 neurons.

566 **Training parameters** Across all three examples, we consider the discounted setting where the
567 discount factor is $\gamma = 0.95$. The learning rate is set to be $\alpha = 0.01$. The number of demonstrated
568 trajectories is set to be 100 in both the random and near-optimal settings.

569 **Reinforcement learning solvers** In order to train the optimal policy, in the gridworld example,
570 we use tabular value-iteration algorithm to learn the Q value of each state action pair. In the snare
571 finding and the TB examples, since the state space is continuous, we apply DDQN to train the Q
572 function and the corresponding policy, where we use a neural network with two intermediate layers
573 each with 64 neurons to represent the function approximators of the Q values. There is one exception
574 in the runtime plot of the snare finding problem in Figure 3(c), where the full Hessian computation is
575 infeasible when a two layer neural network is used. Thus we use an one layer neural network with 64
576 neurons only to test the runtime of different Hessian approximations.

577 C.1 Gridworld Example With Missing Rewards

578 **Problem setup** We consider a 5×5 Gridworld environment with unknown rewards as our MDP
579 problems with unknown parameters. The bottom left corner is the starting point and the top right
580 corner is a safe state with a high reward drawn from a normal distribution $\mathcal{N}(5, 1)$. The agent can
581 walk between grid cells by going north, south, east, west, or deciding to stay in the current grid cells.
582 So the number of available actions is 5, while the number of available states is $5 \times 5 = 25$.

583 The agent collects reward when the agent steps on each individual grid cell. There is 20% chance that
584 each intermediate grid cell is a cliff that gives a high penalty drawn from another normal distribution
585 $\mathcal{N}(-10, 1)$. All the other 80% of grid cells give rewards drawn from $\mathcal{N}(0, 1)$. The goal of the agent
586 is to collect as much reward as possible. We consider a fixed time horizon case with 20 steps, which
587 is sufficient for the agent to go from bottom left to the top right corner.

588 **Training details** Within each individual training step for each MDP problem with missing parame-
589 ters, we first predict the rewards using the predictive model, and then solve the resulting problem
590 using tabular value-iteration. We run in total 10000 iterations to learn the Q values, which are later
591 used to construct the optimal policy. To relax the optimal policy given by the RL solver, we relax
592 the Bellman equation used to run value-iteration by relaxing all the argmax and max operators in
593 the Bellman equation to softmax with temperature 0.1, i.e., we use $\text{SOFTMAX}(0.1 \cdot \text{Q-values})$ to
594 replace all the argmax over Q values. The choice of the temperatue 0.1 is to make sure that the
595 optimal policy is smooth enough but the relaxation does not impact the optimal policy too much as
596 well.

597 **Random and near-optimal trajectories generation** To generate the random trajectories, we have
598 the agent randomly select actions between all actions. To generate the near-optimal trajectories, we
599 replace the softmax with temperature 0.1 by softmax with temperature 1 and train an RL agent using
600 ground truth reward values by 50000 value-iterations to get a near-optimal policy. We then use the
601 trained near-optimal policy to generate 100 independent trajectories as our near-optimal demonstrated
602 trajectories.

603 C.2 Snare Finding Problem With Missing Transition Probability

604 **Problem setup** In the snare finding problem, we consider a set of 20 sites that are vulnerable to
605 poaching activity. We randomly select 20% of the sites as high-risk locations where the probability
606 of having a poacher coming and placing a snare is randomly drawn from a normal distribution
607 $\mathcal{N}(0.8, 0.1)$, while the remaining 80% of low-risk sites with probability $\mathcal{N}(0.1, 0.05)$ having a
608 poacher coming to place a snare. These transition probabilities are not known to the ranger, and the
609 ranger has to rely on features of each individual site to predict the corresponding missing transition
610 probability.

611 We assume the maximum number of snare is 1 per location, meaning that if there is a snare and it
612 has not been removed by the ranger, then the poacher will not place an additional snare there until
613 the snare is removed. The ranger only observes a snare when it is removed. Thus the MDP problem
614 with given parameters is partially observable, where the state maintained by the ranger is the belief of
615 whether a site contains a snare or not, which is a fractional value between 0 and 1 for each site.

616 The available actions for the ranger are to select a site from 20 sites to visit. If there is a snare in
617 the location, the ranger successfully removes the snare and gets reward 1 with probability 0.9, and
618 otherwise the snare remains there with a reward -1 . If there is no snare in the visited site, the ranger
619 gets reward -1 . Thus the number of actions to the ranger is 20, while the state space is continuous
620 since the ranger uses continuous belief as the state.

621 **Training details** To solve the optimal policy from the predicted parameters, we run DDQN with
622 1000 iterations to collect random experience and 10000 iterations to train the model. We use a replay
623 buffer to store all the past experience that the agent executed before. To soften the optimal policy, we
624 also use a relaxed Bellman equation as stated in Section C.2. Because the cumulative reward and the
625 corresponding Q values in this domain is relatively smaller than the Gridworld domain, we replace all
626 the argmax and max operators by softmax with a larger temperature 1 to reflect the relatively smaller
627 reward values.

628 **Random and near-optimal trajectories generation** Similar to Section C.1, we generate the ran-
629 dom trajectories by having the agent choose action from all available actions uniformly at random.
630 To generate the near-optimal trajectories, we replace all the softmax with temperature 1 by softmax
631 with temperature 5, and we use the ground truth transition probabilities to train the RL agent by
632 DDQN using 50000 iterations to generate a near-optimal policy. The near-optimal trajectories are
633 then generated by running the trained near-optimal policy for 100 independent runs.

634 C.3 Tuberculosis With Missing Transition Probability

635 **Problem setup** There are a total of 5 patients who need to take their medication at each time-step
636 for 30 time-steps. For each patient, there are 2 states – non-adhering (0), and adhering (1). The
637 patients are assumed to start from a non-adhering state. Then, in subsequent time-steps, the patients’
638 states evolve based on their current state and whether they were intervened on by a healthcare worker
639 according to a transition matrix.

640 The raw transition probabilities for different patients are taken from [17].¹ However, these raw
641 probabilities do not record a patient’s responsiveness to an intervention. To incorporate the effect
642 of intervening, we sample numbers from $U(0, 0.4)$, and (a) add them to the probability of adhering
643 when intervened on, and (b) subtract them from the probability of adhering when not. Finally, we clip
644 the probabilities to the range of $[0.05, 0.95]$ and re-normalize. We use the raw transition probabilities
645 and the randomly generated intervention effect to model the behavior of our synthetic patients and

¹The raw transition probabilities taken from [17] are only used to generate synthetic patients. The checklist with the published paper will be updated to reflect this change.

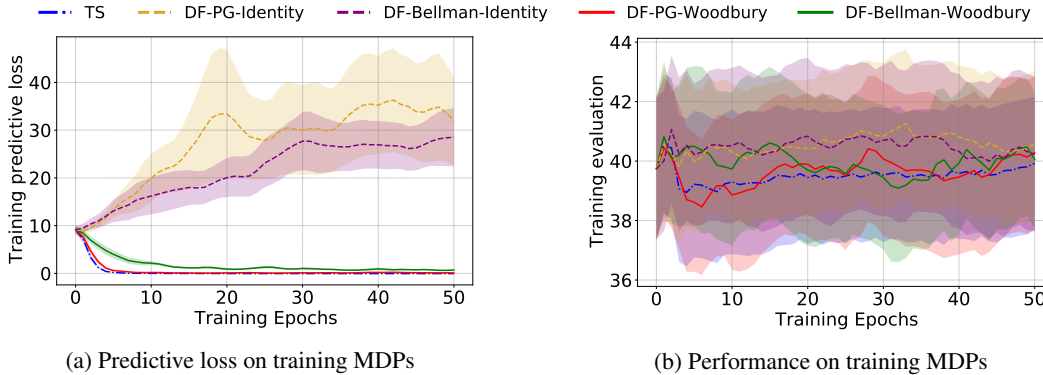


Figure 4: Learning curves of for the TB problem with random trajectories.

646 generate all the training trajectories accordingly. The entire transition matrix for each patient is
 647 then fed as an input to the feature generation network to generate features for that patient. In this
 648 example, we assume the transition matrices to be missing parameters, and try to learn a predictive
 649 model to recover the transition matrices from the generated features using either two-stage or various
 650 decision-focused learning methods as discussed in the main paper.

651 Given the synthetic patients, we consider a healthcare worker who has to choose one patient at every
 652 time-step to intervene on. However, the healthcare worker can only observe the ‘true state’ of a
 653 patient when she intervenes on them. At every other time, she has a ‘belief’ of the patient’s state that
 654 is constructed from the most recent observation and the predicted transition probabilities. Therefore,
 655 the healthcare worker has to learn a policy that maps from these belief states to the action of whom to
 656 intervene on, such that the sum of adherences of all patients is maximised over time. The healthcare
 657 worker gets a reward of 1 for an adhering patient and 0 for a non-adhering one. Like Problem C.2,
 658 this problem has a continuous state space (because of the belief states) and discrete action space.

659 **Training details** Same as Section C.2.

660 **Random and near-optimal trajectories generation** Similar to Section C.2, we generate the ran-
 661 dom trajectories by having the agent choose action from all available actions uniformly at random.
 662 To generate the near-optimal trajectories, we replace all the softmax with temperature 5 by softmax
 663 with temperature 20,² and we use the ground truth transition probabilities to train the RL agent by
 664 DDQN using 100,000 iterations to generate a near-optimal policy. The near-optimal trajectories are
 665 then generated by running the trained near-optimal policy for 100 independent runs.

666 D Additional Experiment Results

667 **Tuberculosis Adherence** The results for this problem can be found in Table 1, and the training
 668 curves can be found in Figure 4. While the standard errors associated with the results *seem* very large,
 669 this is in large part because of the way in which we report them. To keep it consistent with other
 670 problems, we average the absolute OPE scores for each method across multiple problem instances.
 671 However, in the TB case, each problem instance can be very different because the patients in each
 672 of these instances are sampled from the transition probabilities previously studied in [17] that have
 673 diverse patient behaviour. As a result, the baseline OPE values vary widely across different problem
 674 instances, causing a larger variation in Figure 4(b) and contributing as the major source of standard
 675 deviation.

²The reason that we use a relatively larger temperature is because the range of the cumulative reward in TB domain is smaller than the previous two domains. In TB domain, the patients could change from non-adhering back to adhering even if there is no intervention, while in contrast, a snare placed in a certain location will not be removed until the ranger visits the place. In other words, the improvement that intervention can introduce is relatively limited compared to the snare finding domain. Thus even though the cumulative reward in TB domain is larger than the previous two domains, the range is smaller and thus we need a larger temperature.

676 **E Computing Infrastructure**

677 All experiments except were run on a computing cluster, where each node is configured with 2
678 Intel Xeon Cascade Lake CPUs, 184 GB of RAM, and 70 GB of local scratch space. Within each
679 experiment, we did not implement parallelization nor use GPU, so each experiment was purely run
680 on a single CPU core.